INSTITUTE OF PHYSICS PUBLISHING JOURNAL OF PHYSICS: CONDENSED MATTER

J. Phys.: Condens. Matter **17** (2005) 821–836 doi:10.1088/0953-8984/17/6/004

Regeneration of thixotropic magnetic gels studied by mechanical spectroscopy: the effect of the pH

A Ponton[1,4], **A Bee**[2], **D Talbot**[2] **and R Perzynski**[3]

[1] Laboratoire de Biorhéologie et d'Hydrodynamique Physico-chimique, UMR 7057 et Fédération de Recherche Matières et Systèmes Complexes FR2438, Université Paris 7-Denis Diderot, Case 7056, 2 place Jussieu 75251 Paris cedex 05, France
[2] Laboratoire des Liquides Ioniques et Interfaces Chargées, UMR 7612, Université Paris 6-Pierre et Marie Curie, Case 63, 4 place Jussieu 75252 Paris cedex 05, France
[3] Laboratoire des Milieux Désordonnés et Hétérogènes, UMR 7603, Université Paris 6-Pierre et Marie Curie, Case 78, 4 place Jussieu 75252 Paris cedex 05, France

E-mail: ponton@ccr.jussieu.fr

Received 2 September 2004, in final form 4 January 2005
Published 28 January 2005
Online at stacks.iop.org/JPhysCM/17/821

Abstract

Regeneration of thixotropic gels resulting from aggregation of positively charged magnetic nanoparticles is here investigated by mechanical spectroscopy. The frequency independence of the ratio G''/G' (G'' and G' being respectively the viscous and the elastic moduli) at the gel point seen as a liquid–solid transition allows the determination of the gelation time t_g and of the power law exponent on the angular frequency for both moduli ($G' \sim \omega^{\Delta}$, $G'' \sim \omega^{\Delta}$). This behaviour is similar to the one observed for classical chemical and physical gels. It implies a broad relaxation time spectrum which is compatible with previous dynamic magneto-optical birefringence measurements. The value of t_g decreases exponentially with an increase of the pH that controls the interactions between particles through their surface density of charges. In contrast, the relaxation exponent is found to be nearly insensitive to the pH. A fractal dimension of 2.07 ± 0.06 is deduced from the power law exponent Δ at the gelation time.

1. Introduction

Among soft matter studies, lots of works deal with colloidal suspensions which have been the subject of intensive research for a few years. Indeed such materials exhibit a wide range of rheological behaviours and mesoscopic structures can form under weak forces comparable to the thermal energy kT. Individual particles can aggregate to form clusters. Different static and also dynamic structures formed under interparticle interactions can be observed. Under

[4] Author to whom any correspondence should be addressed.

repulsive interactions, a jamming glass transition from a fluid to a disordered solid occurs as the volume fraction increases (Pusey and van Megen 1987, van Megen and Underwood 1994). Under attractive interactions, particles may undergo a sol–gel transition when the range of attraction is short compared to the particle size (Rueb and Zukoski 1997, Yanez *et al* 1999). These two transitions present strong similarities (Segré *et al* 2001). It has been proposed in Weitz and Oliverai (1984) that both of them are dynamic arrest phenomena driven by crowding—of single particles for glass transitions and of fractal clusters for gelation. By molecular dynamics simulations, the local mechanisms of these non-equilibrium transitions from ergodic to non-ergodic states have been identified to arise from a caging of particles for the glass transition and bonding between particles in the case of gelation (Peurtas *et al* 2002). An interpretation has been proposed using mode coupling theory (MCT) for colloidal suspensions with attractive short range interactions (Bergenholtz and Fuchs 1999).

Colloidal gel formation has been widely studied experimentally by means of light scattering and rheology (Poon and Haw 1997, Grant and Russel 1993, Verduin *et al* 1996, Poon *et al* 1997, Krall and Weitz 1998) at various volume fractions of particles and temperatures. In all these studies the attractive interactions are modulated through the nature of the solvent, the temperature, the polymer concentration for sterically stabilized particle systems or addition of a salt for ionic systems. However, only a few works involve magnetic dipolar effects (Butter *et al* 2003a, 2003b). When rigid magnetic dipoles are attached to the particles, both the rotational and translational diffusion of particles (and clusters of particles) are influenced by long range magnetic dipolar interparticle interactions.

We study here by non-invasive mechanical spectroscopy the regeneration of gels of magnetic nanoparticles in which dipolar effects have been evidenced experimentally by small angle scattering experiments (Cousin *et al* 2005). These gels are thixotropic, i.e. they have gel-like properties which disappear on shearing and reappear on standing.

Ferrofluids are colloidal suspensions of magnetic nanoparticles dispersed in a liquid carrier medium (water, oil or organic solvent). Each particle behaves as a small permanent magnet. They interact together through van der Waals and magnetic dipolar interactions. Because of the nanometric size of the particles, collisions with the molecules of the carrier liquid due to Brownian motion are sufficient to prevent sedimentation. However, the energy associated with van der Waals forces and magnetic dipolar ones being of the same order of magnitude as the energy of thermal agitation leads to aggregation of particles. To prevent this aggregation it is necessary to introduce a repulsive barrier between particles. This can be achieved either by the presence of charges on the particle surface leading to electrostatic repulsions which depend on the nature of the counterions or by small chains of adsorbed surfactants leading to steric repulsions (Dubois *et al* 1999).

The ionic ferrofluids studied here are composed of nanoparticles with a maghemite core (γ-Fe_2O_3) dispersed in water. The stability of these aqueous suspensions is here controlled by the modulation of the surface density of the charges of the nanoparticles through pH variations (Hasmonay *et al* 1999) at constant ionic strength and temperature (Dubois *et al* 1999). At the point of zero charge (PZC) located at about pH 7.3, the net surface charge on the particles is zero. At this point, the electrostatic repulsions between uncharged particles do not exist any longer and particles flocculate. Under acidic conditions (pH $<$ PZC), protonation of surface hydroxyl groups leads to a positive surface, while their deprotonation leads to a negative surface under alkaline conditions (pH $>$ PZC). On increasing (pH $<$ PZC) or decreasing (pH $>$ PZC) the pH values, different states are observed for the suspension (Hasmonay *et al* 1999): a *sol state* (acidic or alkaline), a *thixotropic gel state* (acidic or alkaline) which flows under gentle shaking and gels if left at rest and a *floc state*. In this later state the nanoparticles agglomerate and flocculate forming large structures which sediment at the bottom of the experimental cells.

The sol and the gel states have been previously probed locally by dynamic magneto-optical birefringence measurements (Hasmonay *et al* 1999). In a shaken thixotropic gel going from a fluid back to a gel at a given pH, it has been shown that the birefringence intensity can be fitted by a stretched exponential function $I(t) = I_0 \exp[-(t/\tau_E)^{\alpha}]$. The relaxation time τ_E goes through a maximum during the gel regeneration. It has been explained by a first progressive growing of the clusters from a hydrodynamic radius of the order of 100 nm up to 250 nm. The biggest then progressively trap on a macroscopic cluster. Simultaneously the stretched exponent α diminishes to a constant value of about 0.35 which can be interpreted as the signature of a very wide distribution of relaxation times in the system.

Dipolar effects in these magnetic colloidal systems have also been studied by means of small angle x-ray scattering (SAXS) and small angle neutron scattering (SANS) (Cousin *et al* 2005). It was shown that pretransitional aggregated sols can be described as a gas of individual chains of fractal dimension $d_f = 1.62 \pm 0.03$ with a low average number of particles per chain ($\leqslant 5$). Thixotropic gels and flocs present the same pH-independent local fractal dimension d_f. The same fractal dimension is also found for frozen thixotropic gels and fluidized ones. The local structure of the thixotropic gels is not modified by a preshearing that fluidizes the system.

This local probing needed to be completed by a macroscopic study of their rheological properties by non-invasive mechanical spectroscopy. The purpose of this paper is then to investigate the effects of the pH on the liquid–solid transition (LST) that the system undergoes as it regenerates after a preshearing.

2. Theoretical background

The formation of large scale structures lies at the origin of this liquid–solid transition (LST) that can be studied by means of rheology.

One of the first methods developed to detect the LST is based on the divergence of rheological properties such as the steady shear viscosity and the appearance of an equilibrium modulus (Adam *et al* 1985). Despite the simplicity of this method, it has however serious disadvantages. Not only does the divergence of the longest relaxation time make the steady shear flow very difficult to obtain but also the LST is detected by an extrapolation. Moreover, this method is invasive in the sense that a constant shear stress (or shear rate) is applied during the formation of weak structures near the LST.

In contrast, dynamic mechanical spectroscopy is more appropriate for studying the gradual evolution of the material because of the observed universal pattern of the relaxation time spectrum at the LST. Indeed molecular motions are coupled over a wide range of timescales near the LST which can be described as a power law distribution of relaxation times. The relaxation of the shear stress modulus $G(t)$ defined as the ratio $\sigma(t)/\gamma_0$ of the shear stress response $\sigma(t)$ of the material to an imposed small step shear strain γ_0 is then described at the LST by a power law (Chambon and Winter 1987):

$$G(t) = St^{-\Delta} \qquad \lambda_0 < t < \infty \tag{1}$$

where S is the gel stiffness, λ_0 is a lower time cut-off and Δ is a temporal exponent characteristic of the relaxation of the shear stress modulus.

The lower time cut-off λ_0 is the shortest time of the power law behaviour due for example to entanglement effects in polymeric gels (de Rosa and Winter 1994) with typical values between 10^{-7} and 10^{-4} s (Winter 1991).

The theoretical relaxation exponent is restricted to values ranging from 0 and 1 to ensure a finite value of the shear stress modulus at long times ($\Delta > 0$) and the divergence of the low shear viscosity at the LST ($\Delta < 1$).

Such a power law behaviour has been observed as well in physical gels (Chenite *et al* 2001, Hsu and Jamieson 1993, Lin *et al* 1991, Michon *et al* 1993, Ming *et al* 1997, te Nijenhuis and Winter 1989, Power *et al* 1998, Richtering *et al* 1992, Sato *et al* 2000, Takanata *et al* 2002), in organic and inorganic chemical gels (de Rosa and Winter 1994, de Rosa *et al* 1997, Hess *et al* 1998, Koike *et al* 1996, Mours and Winter 1996, Ponton *et al* 1999, Venkataramann and Winter 1990, Vlassopoulos *et al* 1998, Winter and Chambon 1986, Winter 1987) and in colloidal gels (Cocard *et al* 2000).

In mechanical spectroscopy, the storage $G'(\omega)$ and loss $G''(\omega)$ moduli are determined by applying an oscillatory shear stress and measuring an oscillatory shear strain. In the framework of linear viscoelasticity $G'(\omega)$ and $G''(\omega)$ are related to $G(t)$ by

$$G'(\omega) = \omega \int_0^\infty G(t) \sin \omega t \, \mathrm{d}t \tag{2}$$

$$G''(\omega) = \omega \int_0^\infty G(t) \cos \omega t \, \mathrm{d}t. \tag{3}$$

By inserting the expression for $G(t)$ at the LST (equation (1)) in equations (2) and (3), the following expressions for $G'(\omega)$ and $G''(\omega)$ are obtained at the LST:

$$G'(\omega) = \frac{S\pi\omega^\Delta}{2\Gamma(\Delta)\sin(\Delta\pi/2)} \tag{4}$$

$$G''(\omega) = \frac{S\pi\omega^\Delta}{2\Gamma(\Delta)\cos(\Delta\pi/2)} \tag{5}$$

where Γ is the gamma function.

It can be then deduced that the ratio $G''(\omega)/G'(\omega)$ does not depend on frequency at the LST:

$$G''(\omega)/G'(\omega) = \tan(\Delta\pi/2). \tag{6}$$

Therefore the variation of the ratio $G''(\omega)/G'(\omega)$ as a function of time (i.e. during the LST) presents an intersection point which defines the gelation time t_g.

Another quantity of interest is the complex viscosity η^*. Taking into account the above expressions, we obtain

$$|\eta^*| = (1/\omega)(G'^2 + G''^2)^{1/2} = \frac{S\pi\omega^{\Delta-1}}{\Gamma(\Delta)\sin\Delta\pi}. \tag{7}$$

Equation (7) will be used to compute the gel stiffness S from the measurements of $G'(\omega)$ and $G''(\omega)$ at the LST.

The power law behaviour (equation (1)) means a broad relaxation time spectrum without any characteristic time; the critical gel (the gel at the LST) can be described as a fractal structure.

By analogy with polymers, a cluster having a mass M and a radius of gyration R is characterized by a fractal dimension d_f defined by

$$M \sim R^{df}. \tag{8}$$

Different relationships between the critical exponent Δ and the fractal dimension d_f have been proposed. In the case of non-entangled monodisperse polymer fractals described by Rouse dynamics including excluded volume interactions, the relation is (Muthukumar 1985, Martin *et al* 1989)

$$\Delta = d_f/(d_f + 2). \tag{9}$$

Muthukumar (1989) introduced screening effects. In the case of full screening excluded volume, the most complete relation between Δ and d_f is

$$\Delta = 3(5 - 2d_f)/2(5 - d_f). \tag{10}$$

The possible values of Δ ($0 < \Delta < 1$) lead in the framework of this model to a fractal dimension d_f between 1.25 and 2.5; the larger Δ, the lower d_f.

Equation (10) will be used in this study to compute the fractal dimension of the colloidal network.

3. Experimental section

3.1. Materials

3.1.1. Ferrofluid synthesis and characterization. Magnetic nanoparticles of maghemite (γ-Fe_2O_3) are synthesized according to a method described elsewhere (Bée *et al* 1995, Massart 1981). There are two basic steps for the formation of a ferrofluid: synthesis of the magnetic particles and suspension in a liquid carrier with an appropriate treatment of the surface. Particles are obtained by a precipitation reaction that occurs upon mixing an aqueous mixture of $FeCl_2$ and $FeCl_3$ with concentrated ammonium hydroxide. The resulting magnetite (Fe_3O_4) is then stirred in nitric acid, oxidized in maghemite by a boiling solution of ferric nitrate and, after washing, dispersed into water, leading to an ionic acidic ferrofluid. Particles are positively charged with nitrate (NO_3^-) counterions. The pH value of the resulting suspension is about 2.

The particle size distribution of individual nanoparticles is obtained from magnetic measurements on dilute liquid dispersions (volume fraction less than 1%) at pH = 2. It is approximated by a log-normal law (Bacri *et al* 1986). A two-parameter fit of the magnetization curve allows us to determine the mean diameter $d_0 = 7.1$ nm ($\ln d_0 = \langle \ln d \rangle$) and the distribution width $\sigma = 0.4$ (Cabuil and Perzynski 1996).

3.1.2. Thixotropic gel preparation and macroscopic observations. A dilute acidic ferrofluid is prepared. The value of the volume fraction Φ determined from chemical titration of iron (Charlot 1966) is 1.5%. Its osmotic pressure is about 30 Pa and the ionic strength is of the order of 10^{-2} mol l^{-1}.

Many thixotropic gels (see table 1) are prepared from this dilute acidic ferrofluid by adjusting the pH value of the sample with tetramethylammonium hydroxide (TMAOH). In the range of pH studied ($2.70 < \text{pH} < 4.10$), particles bear a positive surface density of charges ranging typically from 20 μC cm^{-2} at pH $\sim$ 2 down to 10 μC cm^{-2} at pH $\sim$ 4. All thixotropic gels are macroscopically homogeneous without syneresis. They do not flow if they are left to stand but fluidize under gentle mechanical shaking.

An initial estimate of the gelation time is made for the different samples after a mechanical shaking for 1 min with a Janke & Kunkel VF2 device set at maximum speed. We measure the time necessary for a given sample to be completely frozen, the test being that the sample can no longer flow. A decrease of the gelation time from several hours to a few minutes on increasing pH value from 3 to 4 is observed, similar to what was observed in Hasmonay *et al* (1999).

3.1.3. Rheological measurements. The experimental apparatus is a stress controlled rheometer (Haake RS150). A cone and plate geometry (60 mm in diameter and 2° in angle) is used for all samples. The temperature control is ensured by water circulation from a thermostated bath and maintained constant at $T = 20.0\,^{\circ}\text{C}$. The samples are mechanically

Table 1. Values of the pH, gelation time, relaxation exponent, fractal dimension, elastic and loss moduli at the gelation time as a function of the pH at different conditions of preshearing: 0.5, 0.3 and 0.7 Pa/1 min.

Samples	pH	t_g (s)	Δ	d_f	G'_{t_g} (Pa)	G''_{t_g} (Pa)
1	2.71	—	—	—	—	—
			0.5 Pa/1 min			
2	3.02	22 560	0.26	2.26	0.62	0.23
3	3.05	31 700	0.37	2.15	0.60	0.39
4	3.09	10 975	0.38	2.14	0.56	0.32
5	3.21	11 700	0.54	1.96	0.17	0.18
6	3.34	9 400	0.40	2.11	0.41	0.24
7	3.43	6 500	0.50	2.00	0.59	0.55
8	3.46	3 600	0.53	1.97	0.21	0.21
9	3.51	3 450	0.25	2.28	1.44	0.51
10	3.57	4 950	0.52	1.98	0.17	0.15
11	3.86	740	0.31	2.21	1.18	0.54
12	3.88	690	0.44	2.06	0.57	0.53
13	4.07	420	0.41	2.11	1.08	0.46
			0.3 Pa/1 min			
2	3.02	20 500	0.53	1.96	0.21	0.21
3	3.05	36 300	0.38	2.14	1.51	0.89
5	3.21	10 300	0.60	1.87	0.12	0.15
11	3.86	910	0.46	2.05	0.32	0.25
12	3.88	1 020	0.38	2.14	0.73	0.46
13	4.07	460	0.30	2.14	1.40	0.70
			0.7 Pa/1 min			
2	3.02	19 675	0.53	1.96	0.29	0.20
3	3.05	19 600	0.35	2.17	0.60	0.39
5	3.21	12 400	0.57	1.91	0.24	0.20
11	3.86	990	0.56	1.93	0.18	0.19
12	3.88	960	0.45	2.06	0.47	0.37

shaken for 1 min using a Janke & Kunkel VF2 device set at maximum speed in order to allow them to be loaded easily onto the plate of the rheological geometry.

Rheological measurements consist of small amplitude oscillations with a strain amplitude of 0.1 Pa within the linear viscoelasticity domain. The frequency applied range is 0.1–1 Hz.

3.1.4. Conditions of preshearing. Before each frequency sweep, the sample is sheared at a constant shear stress σ_{presh} for a time t_{presh}. The amplitude of the preshearing σ_{presh} is varied from 0.3 to 1.0 Pa and the time of preshearing t_{presh} ranges from 60 to 1800 s. The variation of the elastic modulus G' as a function of time at various amplitudes of the preshearing σ_{presh} ($t_{\text{presh}} = 60$ s) for sample 12 (pH = 3.88) is given in figure 1. Whatever σ_{presh} is, G' increases abruptly with time and tends to a nearly constant value with a superimposition of all the curves at long time. This behaviour reflects the building of large structures on long scales. However, it is clearly seen that, at low times, the values of G' associated with $\sigma_{\text{presh}} = 1$ Pa are notably higher than the ones for lower σ_{presh} (0.3, 0.7 Pa). The inset of figure 1 illustrates, for $t = 200$ s, that there is a critical shear stress σ^* above which the preshearing tends to accelerate the gel formation making the initial state of the material not reproducible. This

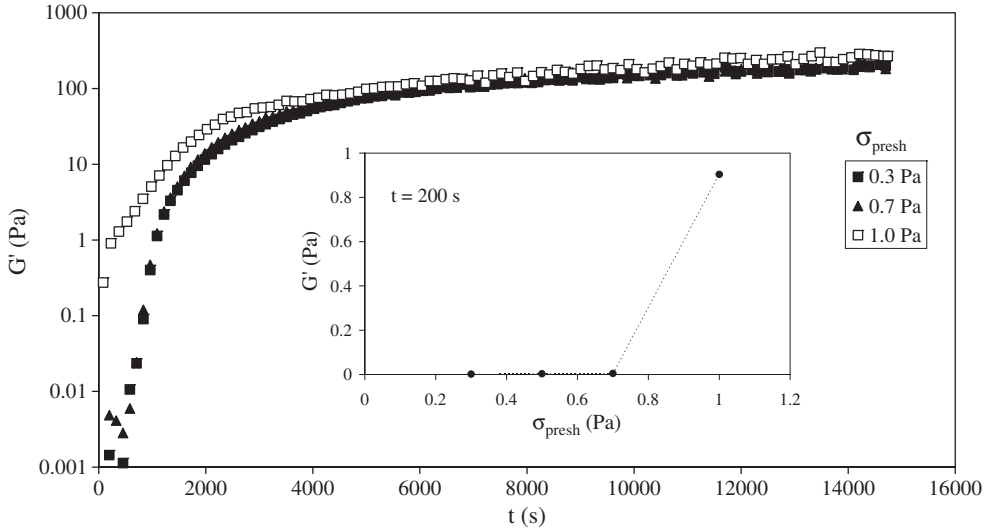

Figure 1. Variation of the elastic modulus G' as a function of time at different amplitudes of preshearing for sample 12. Inset: values of the elastic modulus at 200 s as a function of the amplitude of preshearing σ_{presh}.

behaviour becomes more pronounced as the gelation time is shortened. Hence the values of σ^* are found to decrease as pH increases. The same behaviour is observed at large time of preshearing t_{presh} (those results are not shown). As long as t_{presh} is less than 600 s in the range of σ_{presh} investigated here, the initial state of the flowing liquid is not modified. In consequence, the following conditions of preshearing have been chosen: $\sigma_{\text{presh}} \leqslant 0.7$ Pa and $t_{\text{presh}} = 60$ s, leading to the same initial liquid state for all the samples.

4. Results

An example of the time evolution of G''/G' is shown in figure 2 for sample 5 (pH = 3.21). For each frequency, three time regimes can be distinguished in the dynamical evolution of the moduli.

- In a first time regime, G''/G' decreases slowly with time and decreases also as frequency increases at constant time (see the inset on the left of figure 2 where the values of the ratio G''/G' at 8000 s are reported as a function of frequency). This behaviour is typical of a viscoelastic liquid.

  It should be pointed out that for the lowest frequency (0.1 Hz), a smooth maximum of G''/G' is observed. This maximum is more pronounced for samples with a shorter gelation time. As stated in the introduction, a similar phenomenon has been observed for the relaxation time in birefringence measurements and has been attributed to the initial growth of clusters before forming a macroscopic network. This maximum was also observed in rheological measurements during the gelation of tetraethoxysilane (Hodgson and Amis 1990) and chemical gelation of end-linking polymer (Takahashi *et al* 1994).
- In a second time regime, the decrease is more pronounced and all the curves intersect together at the same point. Its abscissa on the horizontal axis defines the gelation time (sample 5, $t_g = 11\,700$ s). The relaxation exponent ($\Delta = 0.54$) is deduced from the value

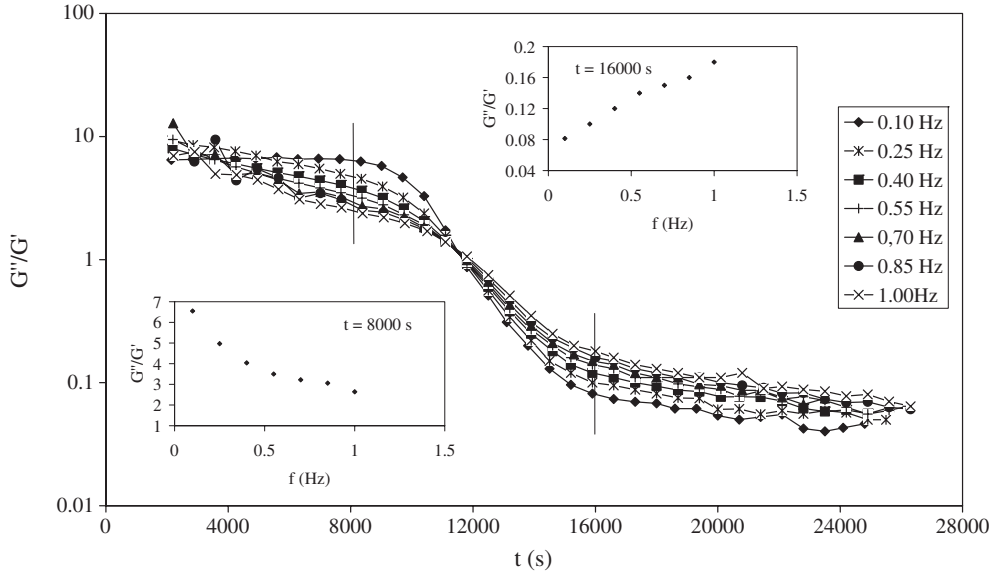

Figure 2. Variation of the ratio of viscoelastic moduli G''/G' as a function of time at different frequencies for sample 5. The two insets display the variation of the ratio G''/G' as a function of frequency before ($t = 8000$ s) and after ($t = 16\,000$ s) the gelation time.

of the ratio G''/G' at t_g using equation (6). During this second time regime, macroscopic structures are formed corresponding to the gel as probed by mechanical spectroscopy. The frequency independence of G''/G' at t_g (equation (6)) is linked to a wide distribution of relaxation times in the system.

- Finally the decrease continues in a third time regime during which the ratio G''/G' increases as frequency increases. It is usual for a viscoelastic solid (see the inset on the right of figure 2 where the values of the ratio G''/G' at 16 000 s are reported as a function of frequency).

The variation of the gelation time t_g as a function of pH is given in figure 3 for three different amplitudes of the preshearing σ_{presh} smaller than σ^*. σ_{presh} has no obvious influence on t_g. This corroborates the assertion that the preshearing in the range investigated has no substantial effect on the gelation process (cf figure 1). The decrease of the gelation time t_g as a function of pH is related to a decrease of the net surface charge of the nanoparticles with increasing pH. Indeed the particle–particle electrostatic repulsion is diminished, leading to a faster aggregation. This decrease of t_g is found to be well described by an exponential law (see the inset in figure 3): $t_g \propto \exp(-3.9\ \mathrm{pH})$.

Whatever the pH, the elastic modulus at the gelation time G'_{t_g} (table 1) is higher than the viscous modulus G''_{t_g} (G''_{t_g}/G'_{t_g} is constant and less than 1).

If the gelation time depends strongly on the pH, we do not observe any tendency for the relaxation exponent Δ, which ranges from 0.25 to 0.54 with a mean value of 0.44 (table 1). The value of Δ could be related to the fractal dimension of the network at the gelation time t_g (equation (10)).

Indeed, the fractal dimension d_f determined from equation (10) in the framework of Muthukumar is also found to be pH independent, as shown in figure 4. We obtain $d_f = 2.07 \pm 0.06$.

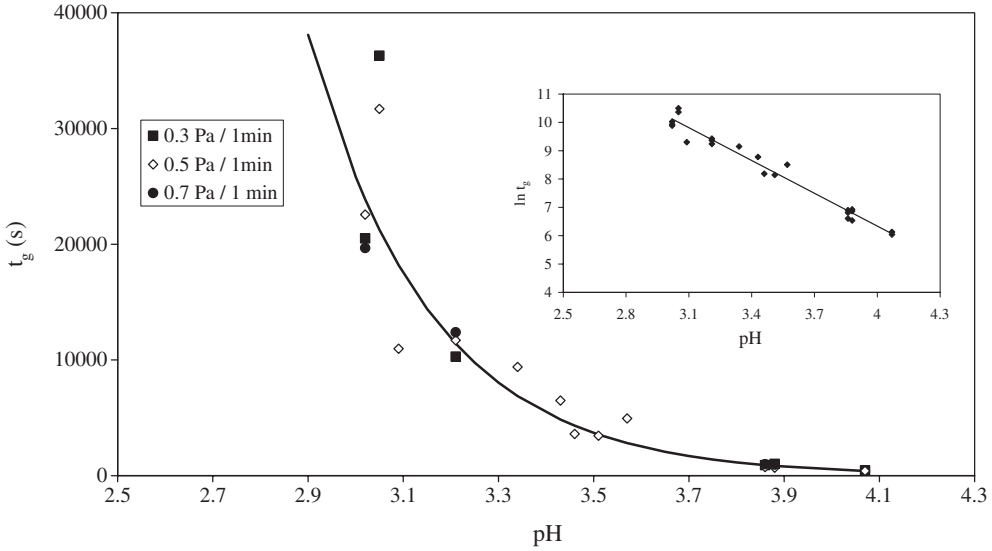

Figure 3. Variation of the gelation time as a function of pH for the different amplitudes of preshearing. The inset displays these results and the fit in a semilogarithmic representation: $t_g \propto \exp(-3.9\ \mathrm{pH})$.

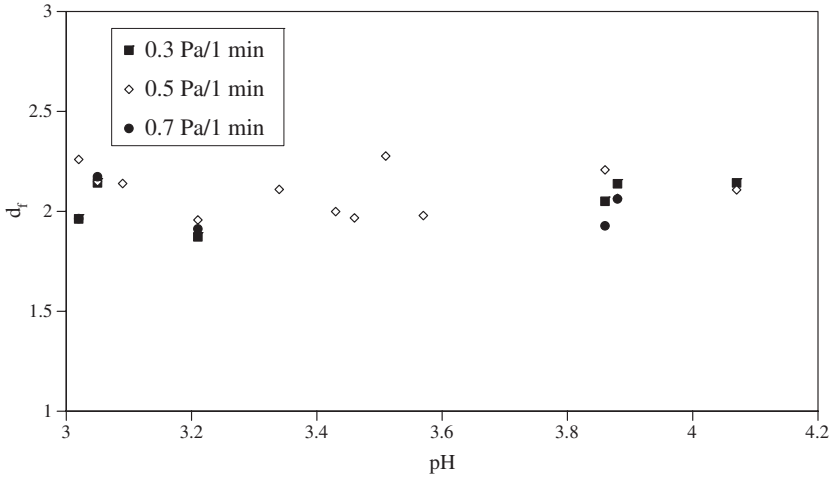

Figure 4. Variation of the fractal dimension d_f determined from equation (10) as a function of pH for the different amplitudes of preshearing. The mean value of d_f is 2.07 ± 0.06.

Using equation (7), it is then also possible to deduce the gel stiffness S. As is shown in figure 5 we find that S and the relaxation exponent Δ are also coupled in our systems although they are not monotonically pH dependent. The gel stiffness has been shown to depend on strand length between cross-linking in the case of irreversible gels by the end-linking reaction of stoichiometrically balanced chemical gels (Chambon *et al* 1986). Nevertheless, the physical meaning of this parameter is not perfectly clear at the present time. A dimensional analysis of S (Pa s^{Δ}) shows that it involves a material characteristic modulus and a time. Experiments on

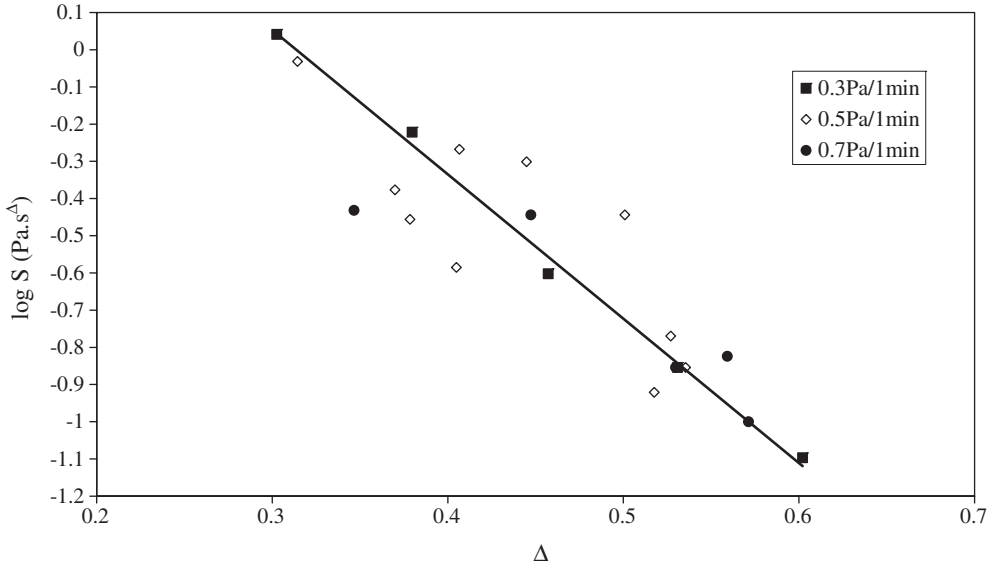

Figure 5. Semilogarithmic variation of the gel stiffness S as a function of the relaxation exponent Δ. The full line is a linear regression of the data points corresponding to $S = G_0\lambda_0^{\Delta}$ with $G_0 \sim 16$ Pa and $\lambda_0 \sim 1$ ms.

a wide range of polydimethylsiloxane cross-linking systems lead Scanlan and Winter (1991) to the proposal of the following relationship:

$$S = G_0\lambda_0^{\Delta} \tag{11}$$

where G_0 and $\eta_0 = G_0\lambda_0$ were very close to the modulus of the fully cross-linked material and the zero-shear viscosity of the prepolymer respectively.

A least-squares fit of the data of the figure 5 gives $G_0 = 16$ Pa and $\lambda_0 \sim 1$ ms. The modulus G_0 characteristic of the material is homogeneous to an energy per volume unit. It is found here to be between the modulus G' at t_g ($G'_{t_g} \approx 1$ Pa) and the osmotic pressure of the initial solutions ($\Pi \approx 30$ Pa). The low time cut-off is found to be 10^3 times larger than the relaxation time of individual nanoparticles (a few microseconds). In contrast, it is of the same order of magnitude as the relaxation time of the clusters of particles measured in a presheared thixotropic gel (Hasmonay *et al* 1999). The product $G_0\lambda_0$ leads to a viscosity $\eta_0 = 16$ mPa s, larger than that (a few mPa s) measured independently for a sol (sample 1, pH = 2.71). It should correspond to the viscosity of the dispersion of individual clusters of the fluidized gels.

Let us now analyse the absolute variations of the elastic modulus G' as a function of time. These variations $G'(t)$ are presented at different pH values in figure 6. For a given pH the elastic modulus increases continuously with time, first abruptly around t_g and then more slowly without reaching a stationary value. This continuous evolution of G' for $t > t_g$ indicates slow relaxations inside the gel associated with restructurings after the gelation time that should be due to the finite lifetime of links between particles or clusters and may lead to ageing properties. The time evolution of G' for a sol (sample 1, pH = 2.71) and for a thixotropic gel (sample 8, pH = 3.46) are given for comparison in the inset of figure 6. In the sol sample, whatever t is, G' always remains much smaller than the mean value of G' in a gel at t_g ($G'_{t_g} \approx 1$ Pa). Moreover, the reduced representation of figure 7 plots G' as a function of t/t_g for samples 4 to 13, an enlargement of the master curve in the vicinity of $t = t_g$ being given in the inset.

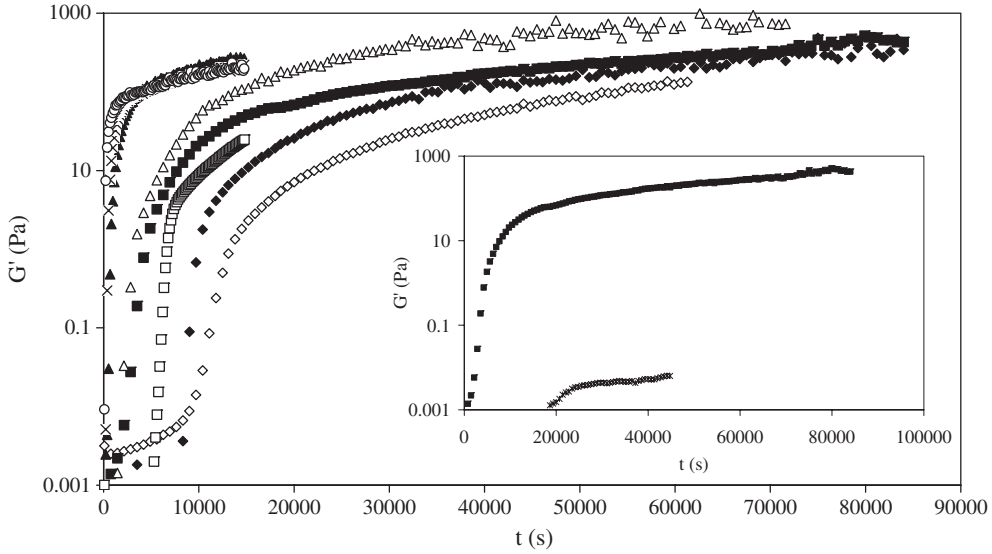

Figure 6. Variation of the elastic modulus as a function of time at different pH values (◇ pH = 3.21, ◆ pH = 3.34, □ pH = 3.43, ■ pH = 3.46, △ pH = 3.51, ▲ pH = 3.86, × pH = 4.07, ○ pH = 4.26). The inset compares $G'(t)$ for sample 1 (∗ pH = 2.71) which always remains a sol and for sample 8 (■ pH = 3.46) which undergoes the sol–gel transition.

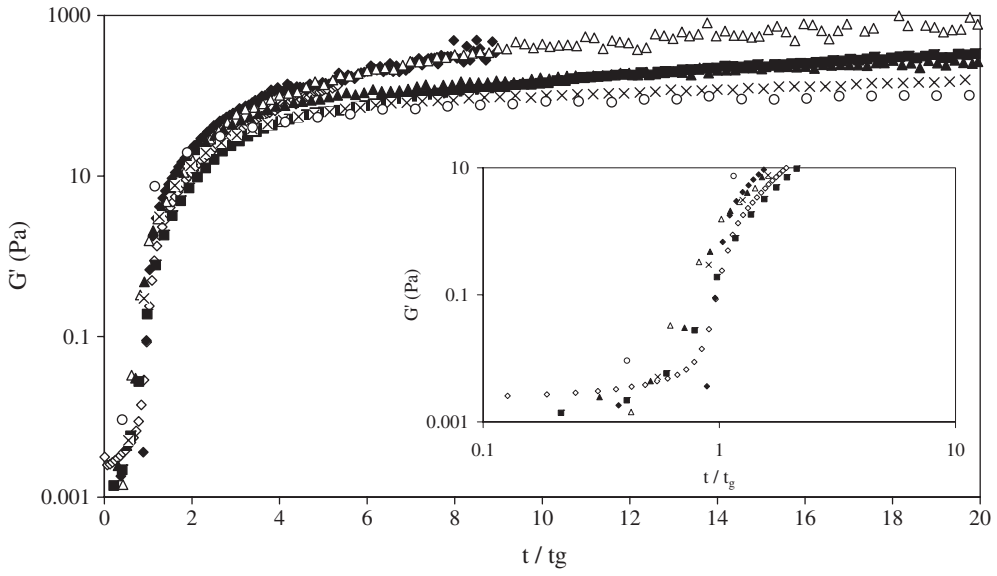

Figure 7. Variation of the elastic modulus as a function of the reduced time t/t_g. The symbols are the same as in figure 6. The inset presents an enlargement of the results in the vicinity of t_g.

Varying the pH thus implies an effect on the gelation time t_g but not on the value of G' at a given t/t_g. This is consistent with the nearly pH-independent values of the relaxation exponent Δ and the fractal dimension d_f at the gelation time, thus with a nearly pH-independent structure.

5. Discussion

We would like to discuss here our experimental results in terms of an aggregation process, one of the main underlying questions being: *Is the magnetic dipolar interparticle interaction relevant at the macroscopic scale in the system investigated here by means of rheological measurements?* A former work (Cousin *et al* 2005) has demonstrated, by means of small angle scattering (SAS) on sols and gels, that *at the nanoscopic scale the answer is yes*. However, these former measurements also show that a fluidization of the thixotropic gels has no influence at the nanoscopic scale—either on the structure factor of the system or on its fractal dimension. This is found equal to 1.62 ± 0.03 by means of SAS for a presheared sample as well, for $t \ll t_g$ and $t \gg t_g$. *At the macroscopic scale the question of whether dipolar effects are observable clearly remains open*.

With respect to those former scattering experiments, the present mechanical spectroscopy measurements allow one to determine much more precisely the *gelation time* t_g of the system and to investigate the properties of the *critical gel at* t_g. Let us first sum up briefly our experimental results:

(i) The gelation time t_g varies exponentially with the pH of the system, over a wide range of times from 5 min to 10 h (see figure 3).
(ii) The power law exponent at the LST is found to be independent of the pH and equal to $\Delta = 0.44 \pm 0.06$. That Δ value can be associated through Muthukumar's formalism to a fractal dimension of the critical gel $d_f = 2.07 \pm 0.06$, clearly larger that the one determined at a nanoscopic scale (see figure 4 and table 1) (Cousin *et al* 2005).
(iii) The stiffness parameter S can be related to the characteristics of the system (see figure 5). The value deduced for the short time cut-off λ_0 ($\sim$1 ms) indicates that here the shortest relevant spatial scale is that of the clusters selected by the preshearing and not the individual nanoparticle size. Those initial clusters have a characteristic size of the order of 200 nm as determined by means of magneto-birefringence relaxation (Hasmonay *et al* 1999).

The exponential variation of t_g with the pH (point (i)) indicates that the aggregation process involved in the present experiment is a first-order one. This would mean an aggregation of the small initial clusters (point (iii)) on a macroscopic cluster with an energy barrier, which varies linearly with pH (Hasmonay *et al* 1999). The aggregation process involved is thus a cluster–cluster aggregation, the charge of the individual nanoparticles remaining an important parameter through the influence of the pH on t_g. This point pleads in favour of a reaction limited colloidal aggregation process (see below). Note that the present aggregation process leads to a structure of aggregates which is pH independent, as the exponents Δ and d_f do not depend on pH (point (ii)). We discuss below the value found here for the exponents Δ and d_f.

The relaxation exponent Δ is not universal. For polymeric systems it depends on several parameters that control the long range connectivity such as the molecular weight of the prepolymer, the stoichiometric ratio and the cross-linker concentration (Izuka *et al* 1992, Winter *et al* 1988) and ranges typically from 0.19 to 0.92 (Hodgson and Amis 1991). For chemical gelation of end-linking polymer (Hodgson and Amis 1991, Koike *et al* 1994, Scanlan and Winter 1991, Takahashi *et al* 1994) the critical gel is generally soft and fragile. Then Δ is large ($0.5 \leqslant \Delta \leqslant 1$) and the elastic modulus is smaller than the viscous modulus ($G' < G''$) at t_g. For physical gelation (Lin *et al* 1991, Nyström *et al* 1995, Power *et al* 1998, Richtering *et al* 1992, Sato *et al* 2000), the critical gel is generally stiff. In this case Δ is small ($0 < \Delta \leqslant 0.5$) and the elastic modulus is larger than the viscous modulus ($G' > G''$) at t_g. The present experimental situation is in between, with G' slightly larger than G'' at t_g and $\Delta = 0.44 \pm 0.06$. The critical gel is rather 'stiff' and consistent with the formation of a physical gel at t_g. However,

the system is close to the crossover between the two situations. Let us note that assuming that the viscoelastic properties present at the local scale a power law behaviour, then using equation (10) and the fractal dimension determined by SAS measurements in Cousin *et al* (2005) we would have expected a much weaker gel with $\Delta \approx 0.78$. The present thixotropic gels thus probably do not have the same 'stiffness' at the macroscopic and the nanoscopic scales.

Several models based on scaling concepts such as percolation have been developed to predict the value of Δ. de Gennes proposed an analogy between gelation and electrical networks (de Gennes 1979). It was then shown that the elastic modulus (critical exponent z) scales with the growth of conductivity in a random resistor–insulator network. de Gennes also proposed an analogy between the divergence of the viscosity (critical exponent k) and the divergence in the conductivity in a random superconductor network (de Gennes 1978). Computer simulations of resistor networks (Derrida *et al* 1984) and simulation in a random superconductivity (Hermann *et al* 1984) yield $z = 1.94 \pm 0.1$ and $k = 0.75 \pm 0.04$ respectively. The derived value of Δ ($\Delta = z/(z+k)$) is then 0.72. A percolation based theory in the Rouse approximation predicts an exponent $\Delta = 0.67$ (Martin *et al* 1989).

The fractal dimension d_f obtained here by rheological spectroscopy is lower than the deduced fractal dimension in the framework of percolation ($d_f = (3 - 2\Delta)/\Delta = 2.5$ with $\Delta = 2/3$). It can also be compared to the ones found by numerical simulations for cluster–cluster aggregation, using fractal concepts. Computer simulations have indeed been developed to get a better understanding of both structural and kinetic aspects of the colloidal aggregation process which lead to the formation of fractal systems. Aggregation may be limited either by diffusion or by reaction.

In *diffusion limited aggregation* (DLA), two particles (or clusters) which do not bear any electrostatic charge permanently stick after a few collisions and the sticking probability is equal to unity. A power law growth of the cluster radius is then observed (Martin *et al* 1990). A first class of diffusion limited aggregation has been introduced by Witten and Sander (1981) in which the cluster formation is due to the accretion of single particles onto an aggregate. The growth in the Witten–Sander model being unrealistic for many real colloidal systems, a second class of diffusion limited aggregation between clusters of all sizes (including single particles) that simultaneously diffuse throughout the systems was then proposed (Meakin 1983). From large scale computers simulations, the values of the fractal dimension in three dimensions is $d_f = 1.78 \pm 0.05$ (Jullien *et al* 1984).

In *reaction limited aggregation* (RLA), the sticking probability is less than unity, for example because of a non-null charge on the clusters. Many collisions occur before bonding, to cross the repulsive barrier, yielding an exponential growth of the cluster radius and a fractal dimension of $d_f = 2.10 \pm 0.05$ (Lin *et al* 1990).

In these cluster–cluster aggregation models, only isotropic interactions such as van der Waals attractions are taken into account. In our experimental system, an anisotropic interaction, namely the dipolar magnetic interaction, is also present. DLA simulation work has been extended to also take into account such anisotropic dipolar interactions (Mors *et al* 1987). In the simulation each particle had an attached rigid magnetic dipole oriented by long range dipolar interactions and clusters were allowed to rotate by Brownian diffusion in three dimensions. It was found that the fractal dimension is lowered with respect to that obtained from standard isotropic aggregation, due to the polarizability effects ($d_f = 1.35 \pm 0.08$) in the limit of infinite dipolar interaction parameter, instead of $d_f = 1.78 \pm 0.05$ without anisotropic interaction (Mors *et al* 1987).

Indeed, the local fractal dimension $d_f = 1.62 \pm 0.03$, determined by SAXS and SANS measurements (Cousin *et al* 2005) inside the gels and for the individual chains of the sols is

reduced under the effect of magnetic dipolar interparticle interaction. However, our present macroscopic value of the fractal dimension $d_f = 2.07 \pm 0.06$, obtained by mechanical spectroscopy, is much higher. It reflects most probably a cluster–cluster aggregation of RLA type.

- The aggregation process is sensitive to an intercluster interaction, the fractal dimension found being close to the RLA prediction and t_g being a function of the pH.
- It is not sensitive to the dipolar magnetic interaction, which can be understood as leading to a null, by symmetry, intercluster contribution in zero field, as for the individual chains of the sols (Cousin *et al* 2005).

In summary, the difference in structure between the nanoscopic scale and the macroscopic one evidenced by scattering and the present rheological measurements reveals a two-level aggregation process:

- An interparticle one which leads to the local structure of the dispersed aggregates in the sols and of the individual clusters in the fluidized gels. It is this process which is probed by means of small angle scattering. It is sensitive to all the interparticle interactions, including the magnetic dipolar one.
- An aggregation of the clusters of the fluidized gels, the preshearing selecting their characteristic size, of the order of 200 nm, associated with a relaxation time $\lambda_0 \sim 1$ ms. It is this process which is probed by means of macroscopic rheology. It is only sensitive to the intercluster interactions. At this spatial scale the dipolar magnetic interaction is averaged to zero in zero magnetic field.

In the future, it will be interesting to probe these two aggregation processes under an applied magnetic field to check how they are modified.

6. Conclusion

The dynamics of regeneration of thixotropic gels obtained with ionic ferrofluids based on maghemite nanoparticles with low surface densities of charge is investigated here. The cluster–cluster aggregation of magnetic dipolar particles is probed at a macroscopic scale by non-invasive mechanical spectroscopy. It is shown for the first time to our knowledge that the gel formation has the same frequency spectrum of viscoelasticity as chemical and physical gelation. The gelation time t_g is determined by the time at which the ratio of moduli G''/G' is independent of frequency. This behaviour is a signature of a broad spectrum of relaxation times, as has been previously probed on more local scales by means of dynamic magneto-optical birefringence measurements. It is shown that t_g is an exponentially decreasing function of the pH which controls the surface density of charge of the magnetic particles and thus the dominant particle–particle interactions. The aggregation can be seen at the macroscopic scale as a first-order process associated with the aggregation of the small dispersed clusters of fluidized gels selected during the preshearing. The relaxation exponent is in contrast found to be nearly insensitive to the pH in the range studied, with a mean value ($\Delta = 0.44$) consistent with the formation of physical gels at the gelation time. The value of the fractal dimension ($d_f = 2.07 \pm 0.06$) deduced from the relaxation exponent using the model of Muthukumar is close to the result from the classical model in three dimensions of reaction limited cluster–cluster aggregation ($d_f = 2.1 \pm 0.05$). It is rather higher than the value for a hierarchical particle–cluster aggregation in the presence of infinite dipolar interactions between magnetic moments on the particles ($d_f = 1.35 \pm 0.08$) and that ($d_f = 1.62 \pm 0.03$) found by means

of small angle scattering on similar samples. We thus do not find any evidence of dipolar magnetic effects in our macroscopic rheological measurements.

Further work is in progress studying the influence of particle size, temperature, concentration, ionic strength and magnetic field on the viscoelastic properties of these thixotropic magnetic gels.

References

Adam M, Delsanti M and Durand D 1985 *Macromolecules* **18** 2285
Bacri J-C, Perzynski R, Salin D, Cabuil V and Massart R 1986 *J. Magn. Magn. Mater.* **62** 36
Bée A, Massart R and Neveu S 1995 *J. Magn. Magn. Mater.* **149** 6
Bergenholtz J and Fuchs M 1999 *Phys. Rev.* E **59** 5706
Butter K, Bomans P H, Frederik P M, Vroege G J and Philipse A P 2003a *Nat. Mater.* **2** 88
Butter K, Bomans P H, Frederik P M, Vroege G J and Philipse A P 2003b *J. Phys.: Condens. Matter* **15** S1451
Cabuil V and Perzynski R 1996 *Magnetic Fluids and Applications Handbook* ed B Berkovski (New York: Begell House Inc.) p 22
Chambon F and Winter H H 1987 *J. Rheol.* **31** 683
Chambon F, Petrovic Z S, MacKnight W J and Winter H H 1986 *Macromolecules* **19** 2146
Charlot G 1966 *Les Méthodes de Chimie Analytique* (Paris: Masson) p 737
Chenite A, Buschmann M, Wang D, Chaput C and Kandani N 2001 *Carbohydr. Polym.* **46** 39
Cocard S, Tassin J F and Nicolai T 2000 *J. Rheol.* **44** 585
Cousin F, Bée A, Boué F, Dubois E, Ponton A and Perzynski R 2005 at press
de Gennes P G 1978 *C. R. Acad. Sci.* B **286** 131
de Gennes P G 1979 *Scaling Concepts in Polymer Physics* (Ithaca, NY: Cornell University Press)
de Rosa M E and Winter H H 1994 *Rheol. Acta* **33** 320
de Rosa M E, Mours M and Winter H H 1997 *Polym. Gels Netw.* **5** 69
Derrida B, Stauffer D, Hermann H J and Vannimenus J 1984 *J. Phys. Lett.* **45** L913
Dubois E, Cabuil V, Boué F and Perzynski R 1999 *J. Chem. Phys.* **111** 7147
Grant M C and Russel W B 1993 *Phys. Rev.* E **47** 2606
Hasmonay E, Bée A, Bacri J-C and Perzynski R 1999 *J. Phys. Chem.* B **103** 6421
Hermann H J, Derrida B and Vannimenus J 1984 *Phys. Rev.* B **30** 4080
Hess W, Vilgis T A and Winter H H 1998 *Macromolecules* **21** 2536
Hodgson D F and Amis E J 1990 *Macromolecules* **23** 2512
Hodgson D F and Amis E J 1991 *J. Non-Cryst. Solids* **131** 913
Hsu S and Jamieson A M 1993 *Polymer* **34** 2602
Izuka A, Winter H H and Hashimoto T 1992 *Macromolecules* **25** 2422
Jullien R, Kolb M and Botet R 1984 *J. Phys. Lett.* **45** L211
Koike A, Nemoto N, Takahashi M and Osaki K 1994 *Polymer* **35** 3005
Koike A, Nemoto N, Watanabe Y and Osaki K 1996 *Polym. J.* **28** 942
Krall A H and Weitz D A 1998 *Phys. Rev. Lett.* **80** 778
Lin M Y, Lindsay H M, Weitz D A, Ball R C, Klein R and Meakin P 1990 *Phys. Rev.* A **41** 2005
Lin Y G, Mallin D T, Chien J C W and Winter H H 1991 *Macromolecules* **24** 850
Martin J E, Adolf D and Wilcoxon J P 1989 *Phys. Rev.* A **39** 1325
Martin J E, Wilcoxon J P, Schaefer D and Odinek J 1990 *Phys. Rev.* A **41** 4379
Massart R 1981 *IEEE. Trans. Magn.* **17** 1247
Meakin P 1983 *Phys. Rev. Lett.* **51** 1119
Michon C, Cuvelier G and Launay B 1993 *Rheol. Acta* **32** 94
Ming Yu J, Jérôme R and Teyssié P 1997 *Polymer* **38** 347
Mors P M, Botet R and Jullien R 1987 *J. Phys. A: Math. Gen.* **20** L975
Mours M and Winter H H 1996 *Macromolecules* **29** 7221
Muthukumar M 1985 *J. Chem. Phys.* **83** 3161
Muthukumar M 1989 *Macromolecules* **22** 4656
Nyström N, Walderhaug H and Hansen F K 1995 *Langmuir* **11** 750
Peurtas A M, Fuchs M and Cates M E 2002 *Phys. Rev. Lett.* **88** 098301
Ponton A, Barboux-Doeuff S and Sanchez C 1999 *Colloids Surf.* A **162** 177
Poon W C K and Haw M D 1997 *Adv. Colloid Interface Sci.* **73** 71
Poon W C K, Pirie A D, Haw M D and Pusey P N 1997 *Physica* A **235** 110

Power D J, Rodd A B, Patterson L and Boger D V 1998 *J. Rheol.* **42** 1021
Pusey P N and van Megen W 1987 *Phys. Rev. Lett.* **59** 2089
Richtering H W, Gagnon K D, Lenz R W, Fuller R C and Winter H H 1992 *Macromolecules* **25** 2429
Rueb C J and Zukoski C 1997 *J. Rheol.* **41** 197
Sato T, Watanabe H and Osaki K 2000 *Macromolecules* **33** 1686
Scanlan J C and Winter H H 1991 *Macromolecules* **24** 47
Segré P N, Prassad V, Schofield A B and Weitz D A 2001 *Phys. Rev. Lett.* **86** 6042
Takahashi M, Yokoyama K and Masuda T 1994 *J. Chem. Phys.* **101** 798
Takanata M, Kobayashi T, Hashimoto T and Takahashi M 2002 *Phys. Rev.* E **65** 041401
te Nijenhuis K and Winter H H 1989 *Macromolecules* **22** 411
van Megen W and Underwood S M 1994 *Phys. Rev.* E **49** 4206
Venkataramann S K and Winter H H 1990 *Rheol. Acta* **29** 423
Verduin H, de Gans B J and Dhont J K G 1996 *Langmuir* **12** 2947
Vlassopoulos D, Chira I, Loppinet B and McGrail P T 1998 *Rheol. Acta* **37** 614
Weitz D and Oliverai M 1984 *Phys. Rev. Lett.* **52** 1433
Winter H H 1987 *Prog. Colloid Polym. Sci.* **75** 104
Winter H H 1991 *Mater. Res. Soc. Bull.* (August) 44
Winter H H and Chambon F 1986 *J. Rheol.* **30** 367
Winter H H, Morganelli P and Chambon F 1988 *Macromolecules* **21** 535
Witten T A and Sander J R 1981 *Phys. Rev. Lett.* **47** 1400
Yanez J A, Laarz E and Bergström L 1999 *J. Colloid Interface Sci.* **209** 162